

# Pulse stabilization by high-order dispersion management

J. Moeser

University of Colorado, Boulder, Colorado 80309

I. Gabitov

Theoretical Division, Los Alamos National Laboratory, Los Alamos, New Mexico 87545

C. K. R. T. Jones

University of North Carolina, Chapel Hill, North Carolina 27599

Received June 26, 2002

The stabilizing effects of dispersion management (DM) at second and third order are studied for both single-channel and wavelength-division multiplexed (WDM) systems. We first derive a model for the slow evolution of a pulse in an optical fiber with high-order dispersion management (HODM). For single-channel systems, in contrast with conventional DM with constant third-order dispersion, this equation possesses a stable solution, the ground state for its associated Hamiltonian, which propagates nearly periodically under direct numerical simulation. Improved performance for WDM systems is also observed, as complicated pulse interactions, which can lead to undesirable effects such as frequency shift, are prevented by HODM. © 2002 Optical Society of America

OCIS codes: 060.2330, 190.4370, 190.5530.

For the past decade, the technique of dispersion management (DM) has been remarkably successful in improving performance in optical transmission systems.<sup>1–3</sup> However, because of the frequency dependence of the dispersion, the application of this technique to wavelength-division multiplexed (WDM) systems is not straightforward.<sup>4</sup> Dispersion compensation at a particular frequency does not guarantee appropriate compensation in neighboring frequency channels. A natural way to surmount the difficulty is to manage dispersion at both second and third order.<sup>5–7</sup> This technique, which has already been incorporated into new dispersion slope compensating fibers, achieves dispersion flattening in an average sense and has yielded impressive results.<sup>3,5,8</sup>

In this Letter we derive an approximate model that describes the slow evolution of short pulses in such a system. The pulses under consideration are sufficiently narrow that the model is valid even for single-channel systems. We verify the existence of stable solutions for the slow evolution equation, with numerical simulation of the averaged equation and direct numerical simulation of the full equation. These simulations indicate that for both single-channel and WDM systems, pulses in high-order dispersion management (HODM) fiber links exhibit markedly better performance than in the equivalent conventional DM system with constant third-order dispersion. The evolution of optical pulses in a fiber with DM at second and third order is governed by

$$iE_z + \beta_2(z)E_{tt} + i\beta_3(z)E_{ttt} + \alpha|E|^2E = 0, \quad (1)$$

where  $E$  is the envelope of the electric field,  $\beta_2(z)$  and  $\beta_3(z)$  are dispersion coefficients at second and third order, respectively, and  $\alpha$  is the strength of Kerr nonlinearity. The spatial coordinate is  $z$ , and the temporal coordinate is  $t$ . We consider dispersion coefficients of the form  $\beta_i(z) = \tilde{\beta}_i(z) + \langle\beta_i\rangle$ ,  $i = 2, 3$ , with  $\tilde{\beta}_i(z)$  piecewise constant and periodic with the same period

$L$  and  $\langle\beta_i\rangle$  the average of  $\beta_i(z)$  over the period. We assume that  $\langle\beta_2\rangle > 0$  and  $\langle\beta_3\rangle = 0$ .

Current optical fibers used for HODM are characterized by the dispersion parameter  $D \sim \mathcal{O}(1 \text{ ps/km nm})$ , average dispersion parameter  $\bar{D} \sim \mathcal{O}(10^{-3} \text{ ps/km nm})$ , differential dispersion parameter  $S \sim \mathcal{O}(10^{-1} \text{ ps/km nm}^2)$ , effective core area  $A_{\text{eff}} \sim \mathcal{O}(10 \text{ } \mu\text{m}^2)$ , and nonlinear index coefficient  $n_2 \sim \mathcal{O}(10^{-20} \text{ m}^2/\text{W})$ .<sup>9</sup> Using standard relationships,<sup>10</sup> we translate these parameters into  $\tilde{\beta}_2, \tilde{\beta}_3, \langle\beta_2\rangle$ , and  $\alpha$  with  $\tilde{\beta}_2 \sim \mathcal{O}(1 \text{ ps}^2/\text{km})$ ,  $\tilde{\beta}_3 \sim \mathcal{O}(10^{-1} \text{ ps}^3/\text{km})$ ,  $\langle\beta_2\rangle \sim \mathcal{O}(10^{-3} \text{ ps}^2/\text{km})$  and  $\alpha \sim \mathcal{O}(1/\text{km W})$ . Defining the characteristic lengths  $z_{\tilde{\beta}_2} = t_0^2/|\tilde{\beta}_2|$ ,  $z_{\tilde{\beta}_3} = t_0^3/|\tilde{\beta}_3|$ ,  $z_{\langle\beta_2\rangle} = t_0^2/|\langle\beta_2\rangle|$ , and  $z_{\text{NL}} = 1/\alpha P_{\text{peak}}$ , where  $P_{\text{peak}}$  is the pulse peak power and  $t_0$  is the pulse width, we see that for a pulse of width 1 ps and power 1 mW,  $z_{\tilde{\beta}_2} \sim \mathcal{O}(1 \text{ km}) < z_{\tilde{\beta}_3} \sim \mathcal{O}(10 \text{ km}) \ll z_{\text{NL}} \sim z_{\langle\beta_2\rangle} \sim \mathcal{O}(1000 \text{ km})$ . We define the dimensionless variables  $u = E/\sqrt{P_{\text{peak}}}$ ,  $\xi = z/z_{\tilde{\beta}_2}$ , and  $\tau = t/t_0$ , and we arrive at the following equation:

$$iu_\xi + \tilde{d}_2(\xi)u_{\tau\tau} + i\frac{z_{\tilde{\beta}_2}}{z_{\tilde{\beta}_3}}\tilde{d}_3(\xi)u_{\tau\tau\tau} + \frac{z_{\tilde{\beta}_2}}{z_{\text{NL}}}|u|^2u + \frac{z_{\tilde{\beta}_2}}{z_{\langle\beta_2\rangle}}\langle d_2 \rangle u_{\tau\tau} = 0. \quad (2)$$

Here  $\tilde{d}_2(z) = z_{\tilde{\beta}_2}\beta_2(z)/t_0^2$ ,  $\tilde{d}_3(z) = z_{\tilde{\beta}_3}\beta_3(z)/t_0^3$ ,  $\langle d_2 \rangle = z_{\langle\beta_2\rangle}\langle\beta_2\rangle/t_0^2$ , and  $z_{\tilde{\beta}_2}/z_{\tilde{\beta}_3} \sim 10^{-1}$ ,  $z_{\tilde{\beta}_2}/z_{\text{NL}} \sim z_{\tilde{\beta}_2}/z_{\langle\beta_2\rangle} \sim 10^{-3}$ .

The pulse undergoes rapid shape changes as a result of rapidly varying linear dispersion, but its spectrum varies slowly on the spatial scale of the dispersion map. Using a standard averaging approach,<sup>11,12</sup> we make the transformation

$$u = \mathcal{L}\{A\} = \int_{-\infty}^{\infty} \exp\left(i\omega\left\{\tau - \omega \int_0^\xi [\tilde{d}_2(s')] - \omega(z_{\tilde{\beta}_2}/z_{\tilde{\beta}_3})\tilde{d}_3(s')\right\}ds'\right) \hat{A}d\omega \quad (3)$$

and arrive at the equation for the slow evolution of the spectrum  $\hat{A}(\xi, \omega)$ :

$$i\hat{A}_\xi - \frac{z_{\tilde{\beta}_2}}{z_{\langle\beta_2\rangle}} \langle d_2 \rangle \omega^2 \hat{A} + \frac{z_{\tilde{\beta}_2}}{z_{\text{NL}}} \int_{-\infty}^{\infty} \delta(\omega - \omega_1 + \omega_2 - \omega_3) \\ \times \Theta(\Delta_2, \Delta_3) \hat{A}(\xi, \omega_1) \hat{A}^*(\xi, \omega_2) \hat{A}(\xi, \omega_3) d\omega_1 d\omega_2 d\omega_3 = 0, \\ \Theta(\Delta_2, \Delta_3) = \frac{1}{L} \int_0^L \exp \left[ i\Delta_2 \int_0^\xi \tilde{d}_2(s') ds' \right. \\ \left. - i\Delta_3 \left( \frac{z_{\tilde{\beta}_2}}{z_{\tilde{\beta}_3}} \right) \int_0^\xi \tilde{d}_3(s') ds' \right] d\xi,$$

where  $\Delta_2 = \omega^2 - \omega_1^2 + \omega_2^2 - \omega_3^2$  and  $\Delta_3 = \omega^3 - \omega_1^3 + \omega_2^3 - \omega_3^3$ . If we consider a symmetric dispersion map  $\tilde{d}_j(\xi) = D_j$  for  $\xi \in [0, \theta)$  and  $\xi \in [L - \theta, L)$ ,  $\tilde{d}_j(\xi) = -D_j$  for  $\xi \in [\theta, L - \theta)$ , and define the map strengths to be  $s_2 = \theta D_2$  and  $s_3 = \theta D_3$ , we may directly compute  $\Theta(\Delta_2, \Delta_3) = 4\theta \sin(s_2 \Delta_2 - s_3 \Delta_3) / L(s_2 \Delta_2 - s_3 \Delta_3)$ .

The averaged equation is the Euler–Lagrange equation for the averaged Hamiltonian:

$$H(A) = \frac{z_{\tilde{\beta}_2}}{z_{\langle\beta_2\rangle}} \langle d_2 \rangle \int_{-\infty}^{\infty} |A_\tau|^2 d\tau \\ - \frac{z_{\tilde{\beta}_2}}{z_{\text{NL}}} \frac{1}{L} \int_0^L \int_{-\infty}^{\infty} |\mathcal{L}\{A\}|^4 d\tau d\xi,$$

where  $\mathcal{L}$  is defined by Eq. (3). We state that this Hamiltonian possesses a ground state, which is smooth, decays rapidly for large  $\tau$ , and propagates stably for the full evolution equation. The ground state is a solution for a nonlinear eigenvalue problem:

$$-\lambda \hat{v} + \frac{z_{\tilde{\beta}_2}}{z_{\langle\beta_2\rangle}} \langle d_2 \rangle \omega^2 \hat{v} + \frac{z_{\tilde{\beta}_2}}{z_{\text{NL}}} \int_{-\infty}^{\infty} \delta(\omega - \omega_1 + \omega_2 - \omega_3) \\ \times \Theta(\Delta_2, \Delta_3) \hat{v}(\omega_1) \hat{v}^*(\omega_2) \hat{v}(\omega_3) d\omega_1 d\omega_2 d\omega_3 = 0,$$

where  $\hat{v}(\omega)$  is defined through  $A(\xi, \tau) = \exp(i\lambda\xi)v(\tau)$  and  $\lambda$  is the minimum value of  $[(z_{\tilde{\beta}_2}/z_{\text{NL}})(1/L) \times \int_0^L \int_{-\infty}^{\infty} |\mathcal{L}\{\xi\}A|^4 d\tau d\xi - (z_{\tilde{\beta}_2}/z_{\langle\beta_2\rangle}) \langle d_2 \rangle \int_{-\infty}^{\infty} |A_\tau|^2 d\tau] / \int_{-\infty}^{\infty} |A|^2 d\tau$  over the class of functions with  $\int_{-\infty}^{\infty} |A_\tau|^2 d\tau < \infty$  and  $\int_{-\infty}^{\infty} |A|^2 d\tau$  fixed. This equation is solved via iteration. The inset in Fig. 1 shows the shape of the ground-state solution for the parameters  $L = 1$ ,  $\tilde{d}_2(\xi) = \tilde{d}_3(\xi) = 5.0$  if  $\xi \in [0, 0.25)$  or  $\xi \in [0.75, 1.0)$ ,  $\tilde{d}_2(\xi) = \tilde{d}_3(\xi) = -5.0$  if  $\xi \in [0.25, 0.75)$ ,  $\langle d_2 \rangle = 1.0$ ,  $z_{\tilde{\beta}_2}/z_{\tilde{\beta}_3} = 1.0$ ,  $z_{\tilde{\beta}_2}/z_{\text{NL}} = z_{\tilde{\beta}_2}/z_{\langle\beta_2\rangle} = 0.1$ . The eigenvalue computed in this case is  $\lambda = 0.38$ . The solution is computed on the time domain  $[-30, 30]$  with 2048 Fourier modes. The logarithm of the amplitude  $|A(\tau)|$  is plotted versus time. One observes a nearly Gaussian central peak, along with many secondary peaks that decay rapidly. This is similar to the structure of the ground states observed for the case  $\beta_3(z) = 0$ ,<sup>12,13</sup> which is also included in the inset for comparison. This ground-state solution can be used as a bit carrier in fiber-optic systems with management of second- and third-order dispersion.

The remainder of this Letter demonstrates the stabilizing effects of HODM. It is well known that, in general,<sup>14</sup> third-order dispersion breaks the time symmetry of the modeling nonlinear Schrödinger equation, deforming pulses and leading to the emission of continuous radiation.<sup>15,16</sup> The green curve in Fig. 1 depicts the solution profile in a single-channel system with constant third-order dispersion. The simulation parameters are  $\tilde{d}_2(\xi) = \tilde{d}_3(\xi) = \pm 1.0$  and  $z_{\tilde{\beta}_2}/z_{\tilde{\beta}_3} = z_{\tilde{\beta}_2}/z_{\text{NL}} = 0.1$  for evolution up to 15  $z$  units, corresponding to an evolution through 150 km of fiber with real fiber units of  $t_0 = 3.5$  ps,  $P_{\text{peak}} = 10$  mW,  $\tilde{\beta}_2 = 1.2$  ps<sup>2</sup>/km,  $\tilde{\beta}_3 = 0.43$  ps<sup>2</sup>/km,  $\langle\beta_2\rangle = 0.12$  ps<sup>2</sup>/km,  $z_{\tilde{\beta}_2} = 10$  km, and  $z_{\tilde{\beta}_3} = z_{\text{NL}} = z_{\langle\beta_2\rangle} = 100$  km. The dispersion map is set up symmetrically as described above. One clearly observes pulse deterioration for conventional DM systems with constant third-order dispersion. However, this destruction is prevented in the system with HODM. The blue curve in Fig. 1 shows the solution profile for a HODM fiber with  $d_3(\xi) = \pm 0.1$  and the same initial data. The use of HODM imposes time symmetry, and the initial profile is nearly recovered after each period of compensation.

The deleterious effect of constant third-order dispersion is even more serious for WDM systems. Pulses propagating in different frequency channels experience different group velocities and inevitably collide. In the presence of constant third-order dispersion, these collisions are inelastic and the individual pulses degrade after each collision. Moreover, if  $\tilde{\beta}_3$  is sufficiently large, the pulses coalesce and propagate as a single formation. Figure 2 shows

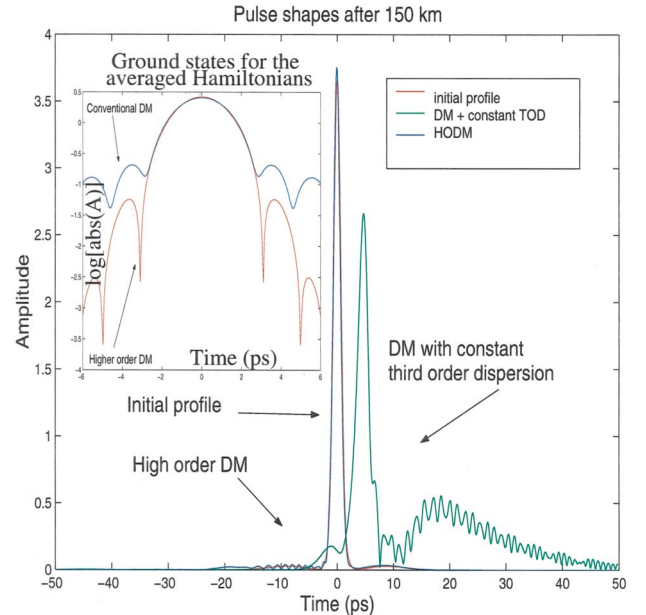


Fig. 1. Stabilization of pulse deterioration. The figure shows snapshots of amplitude profiles of pulses traveling in a DM system with constant third-order dispersion (green curve) and in a HODM system (blue curve). The initial profile is the same for each simulation (red curve). The inset shows the amplitude profiles of the ground states for the averaged Hamiltonians, both with and without inclusion of third-order dispersion.

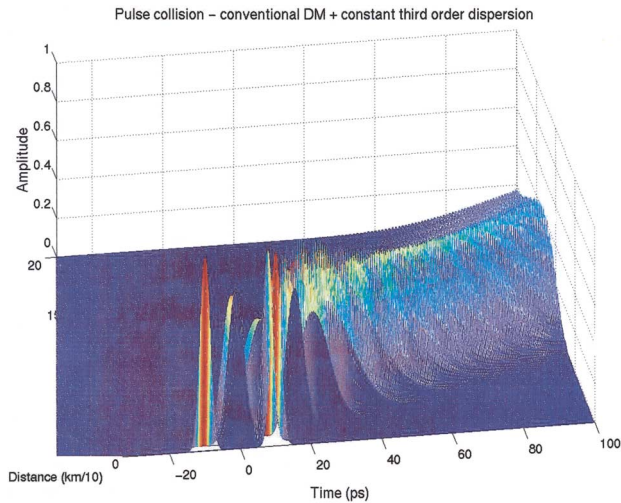


Fig. 2. Pulse collision in a conventional DM fiber with constant third-order dispersion. The figure shows the evolution in the time domain of two pulses that are initially separated in both the time and the frequency domains in a conventional DM fiber with constant third-order dispersion. Snapshots of the amplitude profile were taken every 5 km.

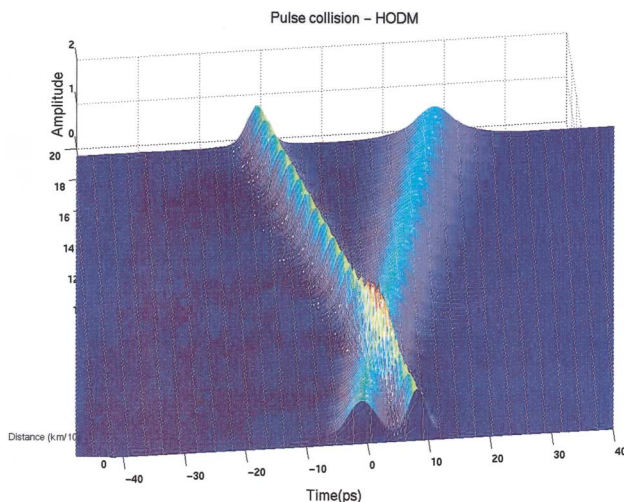


Fig. 3. Pulse collision in a fiber with HODM. The figure shows the evolution in the time domain of two pulses that are initially separated in both the time and the frequency domains in a fiber with HODM. Snapshots of the amplitude profile were taken every 5 km.

the result of a collision of this type. The simulation parameters are the same as those described for the simulation corresponding to Fig. 1. We solve original equation (2) with Gaussian initial pulses separated in the time domain by 20 ps and in the frequency domain by 1 THz. Our numerical results show that HODM fibers can restore an elastic character to the pulse interaction and eliminate the effects of pulse coalescence. Figure 3 shows a pulse collision with the same initial data and parameters as the previous simulation but with management of third-order dispersion. The shapes of the pulse trajectories reveal an elastic character of collision, as pulses separate after collision with no evidence of coalescence. These

results suggest that HODM fibers have great potential to improve performance in WDM systems.

We have provided theoretical and numerical evidence of the existence of stable optical pulses in optical fiber links with second- and third-order dispersion management. We have also demonstrated that the implementation of HODM and the use of these stable pulses as bit carriers can improve performance of both high-speed single-channel systems and WDM data transmission systems.

The support of Los Alamos National Laboratory, U.S. Department of Energy, through contract W-7-405-ENG-36 and its Program in Applied Mathematical Sciences, KJ-01-01, U.S. Army Research Office-Far East (grant N62649-02-1-0004; I. Gabitov) and National Science Foundation grant DMS-0073923 (J. Moeser and C. Jones) is gratefully acknowledged. J. Moeser's e-mail address is moeser@babbage.colorado.edu.

## References

1. F. Favre, D. LeGuen, and T. Georges, *Electron. Lett.* **34**, 1868 (1998).
2. L. F. Mollenauer, P. V. Mamyshev, J. Gripp, M. J. Neubelt, N. Mamysheva, L. Gruner-Nielson, and T. Veng, *Opt. Lett.* **25**, 704 (2000).
3. F. Liu, J. Bennike, S. Dey, C. Rasmussen, H. Mikkelsen, P. Mamyshev, D. Gapontse, and V. Ivshin, in *Optical Fiber Communication Conference (OFC)*, Vol. 70 of OSA Trends in Optics and Photonics Series (Optical Society of America, Washington, D.C., 2002).
4. N. S. Bergano, C. R. Davidson, M. A. Mills, P. C. Corbett, R. Menges, J. L. Zyskind, J. W. Shulhoff, A. K. Srivastava, and C. Wolf, in *Optical Amplifiers and Their Applications*, A. Willner, M. Zervas, and S. Sasaki, eds., Vol. 16 of OSA Trends in Optics and Photonics Series (Optical Society of America, Washington, D.C., 1997), postdeadline paper PD-9.
5. M. Manna and E. A. Golovchenko, in *Optical Fiber Communication Conference*, Vol. 54 of OSA Trends in Optics and Photonics Series (Optical Society of America, Washington, D.C., 2001).
6. E. A. Golovchenko, V. J. Mazurczyk, D. G. Duff, and S. M. Abbott, *IEEE Photon. Technol. Lett.* **11**, 821 (1999).
7. M. Murakami, H. Maeda, and T. Imai, *IEEE Photon. Technol. Lett.* **11**, 898 (1999).
8. L. du Mouza, E. Seve, H. Mardoyan, S. Wabnitz, P. Silard, and P. Nouchi, *Opt. Lett.* **26**, 1128 (2001).
9. G. Shaulov (gshaulov@tycomltd.com; personal communication, August 9, 2001).
10. G. P. Agrawal, *Fiber-Optic Communication Systems*, 2nd ed. (Wiley, New York, 1997).
11. I. Gabitov and S. K. Turitsyn, *Opt. Lett.* **21**, 327 (1995).
12. M. J. Ablowitz and G. Biondini, *Opt. Lett.* **23**, 1668 (1998).
13. J. H. B. Nijhof, N. J. Doran, W. Forysiak, and F. M. Knox, *Electron. Lett.* **33**, 1726 (1997).
14. We note that a stationary solution for the conventional DM equation with constant third-order dispersion was computed numerically by Y. Takushima, X. Wang, and K. Kikuchi, *Electron. Lett.* **35**, 739 (1999).
15. J. N. Elgin, *Opt. Lett.* **17**, 1409 (1992).
16. J. N. Elgin, T. Brabec, and S. M. J. Kelly, *Opt. Commun.* **114**, 321 (1995).